



euronoise

# Interferometric synthetic aperture processing: a comparison of sonar and radar

Michael Hayes and Peter Gough

University of Canterbury, Private Bag 4800, 8022 Christchurch, New Zealand
michael.hayes@canterbury.ac.nz

Interferometric aperture synthesis is an inverse problem that attempts to form an elevation map of the earth (in the case of radar) or a bathymetric map of the seafloor (in the case of sonar). In both cases, a pair of transducers is configured as an interferometer. After aperture synthesis is performed to produce a pair of images, the height of each resolvable scatterer can be estimated using time delay estimation between the image pairs and knowledge of the system geometry.

While interferometric synthetic aperture sonar (InSAS) seems like an obvious extension of the methods of interferometric synthetic aperture radar (InSAR), the height estimation algorithms are surprisingly different. In this paper we start with the principle of generalised correlation for optimal time delay estimation. This filters the signals to maximise their coherence since the accuracy of the time delay estimates, and thus the height estimates, strongly depends upon the signal coherence. We then consider the fundamental differences between InSAR and InSAS; namely the relative signal bandwidth, aperture sampling rate, and geometry and show how application of generalised correlation time delay estimation leads to the differences in how InSAS and InSAR signals are processed.

# 1 Introduction

Interferometric aperture synthesis is an inverse problem that attempts to form an elevation map of the earth (in the case of radar) or a bathymetric map of the seafloor (in the case of sonar).

With single-pass interferometric synthetic aperture radar (InSAR) a pair of antennas are configured as an interferometer, where one of the antennas (or a separate antenna) is used to illuminate the scene (either from a spaceborne or airborne platform). Alternatively, a single transmitter/receiver pair is flown on a similar but displaced track; a technique known as repeat pass interferometry. After pulse compression and synthetic aperture reconstruction (taking care to preserve the phase) two images are obtained $d_1(y,r)$ and $d_2(y,r)$, where $y$ is along-track position and $r$ is slant range. The goal of interferometric processing is to reconstruct a height image $z(x,y)$ where $x$ denotes cross-track position.

In principle, interferometric synthetic aperture sonar (InSAS) is similar to InSAR but with a towed or autonomous sonar platform having a transducer (projector) to ensonify the seafloor and a pair of hydrophone arrays to record the scattered echoes. The arrays of hydrophones are required to increase the along-track sampling rate since the speed of sound propagation is many orders of magnitude slower than electromagnetic propagation. The echoes from each hydrophone array are pulse compressed and combined using synthetic aperture reconstruction algorithms to produce a pair of images. While InSAS height estimation seems like an obvious equivalent to the more mature InSAR, the height estimation algorithms are surprisingly different.

In this paper we start with a simple scattering model and using this model consider the correlation coefficient between the two signals. The height estimation problem is then posed as an optimisation problem where both the time delay and time scaling need to be considered. We show that by ignoring the time scaling that the height reconstruction problem is equivalent to time delay estimation followed by a geometric mapping to infer height. We then consider the principle of generalised correlation for optimal time delay estimation. This filters the signals to maximise their coherence since the accuracy of the time delay estimates, and thus the height estimates, strongly depends upon the signal coherence. Finally, we consider the fundamental differences between InSAR and InSAS; namely the relative signal bandwidth, aperture sampling rate, and geometry and show how application of generalised correlation time delay estimation leads to the differences in InSAS and InSAR processing.

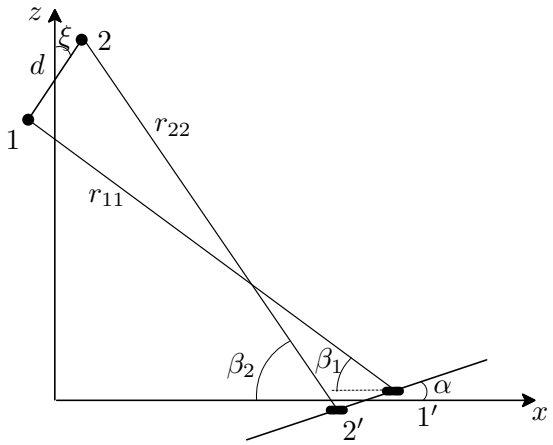


Figure 1: Exaggerated interferometer geometry for two receivers labelled 1 and 2 with corresponding footprints labelled $1'$ and $2'$, and grazing angles $\beta_1$ and $\beta_2$. The interferometer baseline is $d$, the interferometer tilt is $\xi$, and the local terrain slope is $\alpha$.

# 2 Scattering model

Consider an interferometer shown in Figure 1 formed by a pair of receivers located at $(x_1, z_1)$ and $(x_2, z_2)$ with a transmitter at $(x_i, z_i)$. The transducers are side-looking in the $+x$ direction so scattering from the $-x$ direction can be ignored. At a given instant $t$ after a transmission, the pulse-compressed echo signals can be modelled as the superposition of the scatterers at a range $ct/2$. Thus, ignoring trivial amplitude factors and approximating the 2-D scattering by a line integral [1], the baseband pulse-compressed complex envelope signals scattered from a nominally flat seafloor have the form:

$$d_h(t) = \int_{-\infty}^{\infty} \frac{1}{r_h r_i} a(x) p\left(t - \frac{r_h + r_i}{c}\right) \times \exp\left(-\mathrm{j}k_0\left(r_h + r_i\right)\right) \mathrm{d}x. \qquad (1)$$

This is a time-domain simplification of the Kirchhoff scattering model where the subscript $h$ denotes the receiver number, $c$ is the speed of propagation, $p(t)$ is the baseband pulse-compressed signal, $k_0 = 2\pi f_0/c$ is the angular wavenumber of the centre frequency $f_0$, $r_i$ is the range from the source to a scattering point at $(x, z(x))$, while $r_h$ is the range from the scattering point to receiver $h$:

$$r_i = \sqrt{(x - x_i)^2 + (z - z_i)^2}, \quad (2)$$

$$r_h = \sqrt{(x - x_h)^2 + (z - z_h)^2}. \quad (3)$$

Assuming a quasi-monostatic geometry (with the transmitter located near the receivers); that the grazing angles $\beta_h$ are large so that the Kirchhoff approximation is applicable [2]; that the projected pulse length is small compared to the range so that the Fraunhofer approximation is valid; that the surface roughness is small compared to the range resolution; that the local terrain tilt is negligible (this can be modelled by a local coordinate rotation); and ignoring beam pattern effects (these can be modelled as a time-domain convolution since the change in grazing angle over each footprint is small compared to the broad vertical beam pattern), (1) becomes

$$d_h(t) \approx \frac{4}{(ct)^2} \exp\left(-\mathrm{j}2\pi f_0 \left(t - \frac{\bar{x}_h}{c}\eta_{xh}\right)\right) \times \int_{-\infty}^{\infty} a(x) \exp\left(\mathrm{j}k_0 h(x) \eta_{zh}\right) \times p\left(\frac{\bar{x}_h - x}{c}\eta_{xh}\right) \exp\left(-\mathrm{j}k_0 x \eta_{xh}\right) \mathrm{d}x. \quad (4)$$

Here $h(x)$ denotes the local height variation, $(\bar{x}_h, \bar{z}_h)$ denotes the footprint centre for the $h^{\text{th}}$ receiver at each instant $t$, $\bar{\beta}_h = \bar{\beta}_h(t)$ are the scattered grazing angles for each footprint,

$$\cos\bar{\beta}_h = \frac{\bar{x}_h - x_h}{r_{hh}}, \quad (5)$$

$\bar{\beta}_{ih} = \bar{\beta}_{ih}(t)$ are the incident grazing angles,

$$\cos\bar{\beta}_{ih} = \frac{\bar{x}_h - x_i}{r_{ih}}, \quad (6)$$

and $\eta_{xh} = \eta_{xh}(t)$ and $\eta_{zh} = \eta_{zh}(t)$ are the wavenumber scaling factors given by

$$\eta_{xh} = \cos\bar{\beta}_{ih} + \cos\bar{\beta}_h, \quad (7)$$

$$\eta_{zh} = \sin\bar{\beta}_{ih} + \sin\bar{\beta}_h. \quad (8)$$

Despite the many approximations in the derivation (4), it is worth noting that for a given time $t$ after pulse transmission, the echo signals have been scattered from slightly different regions (or footprints), a phenomenon known as the footprint shift. In addition, due to the difference in grazing angle, the footprint sizes (the length of the projections of $p(t)$) are also slightly different.

# 3 Correlation coefficient

A common measure of the similarity between two signals is the correlation coefficient. The correlation coefficient at each instant $t$ as a function of delay $\tau$ between the signals is given by

$$\rho_{12}(t,\tau) = \frac{\mathrm{E}\left[d_2(t) d_1^*(t-\tau)\right]}{\sqrt{\mathrm{E}\left[\left|d_1(t-\tau)\right|^2\right] \mathrm{E}\left[\left|d_2(t)\right|^2\right]}}. \quad (9)$$

Assuming that the scatterers are uncorrelated and uniformly distributed, then the correlation coefficient for a small delay $\tau$ can be expressed as

$$\rho_{12}(t,\tau) = \exp\left(\mathrm{j}\Phi(t)\right) M\left(\frac{f_0}{c}\left(\eta_{x1} - \eta_{x2}\right), \tau\right), \quad (10)$$

where $\Phi(t)$ is the interferometric phase given by

$$\Phi(t) = \exp\left(\mathrm{j}k_0\left(\bar{x}_1\eta_{x1} - \bar{x}_2\eta_{x2}\right)\right), \quad (11)$$

and $M = M(f_x, \tau)$, where

$$M = \frac{\mathcal{F}_x\left\{p\left(\frac{\bar{x}_2 - x}{c}\eta_{x2}\right) p^*\left(\frac{\bar{x}_1 - x}{c}\eta_{x1} - \tau\right)\right\}}{\sqrt{\int_{-\infty}^{\infty}\left|p\left(\frac{\bar{x}_2 - x}{c}\eta_{x2}\right)\right|^2 \mathrm{d}x \int_{-\infty}^{\infty}\left|p\left(\frac{\bar{x}_1 - x}{c}\eta_{x1}\right)\right|^2 \mathrm{d}x}}. \quad (12)$$

Here $\mathcal{F}_x\{.\}$ denotes a Fourier transform over $x$ evaluated at spatial frequencies $f_x$.

Equation (10) shows that to maximise the correlation coefficient, the footprint shift $\bar{x}_1 - \bar{x}_2$ needs to be compensated (except for the scattering point on the interferometer axis where the footprint shift is zero). It also shows that the correlation is never perfect due to the slight difference in look angle resulting in $\eta_{x1} \neq \eta_{x2}$. This slight scaling of the footprints results in baseline decorrelation. For example, if the compressed pulse has the form $p(t) = \mathrm{rect}\left(t/T_p\right)$ then the maximum correlation can be approximated by [1]

$$\max\left\{\rho_{12}\right\}(t) \approx \exp\left(-\mathrm{j}k_0 \frac{D}{2} \sin\left(\bar{\beta} - \xi\right)\right) \times \mathrm{sinc}\left(\frac{f_0 T_p D}{H} \sin\bar{\beta} \tan\left(\bar{\beta} + \alpha\right) \cos\left(\bar{\beta} - \xi\right)\right), \quad (13)$$

where $\xi$ is the tilt of the interferometer axis, $D = d/2$ is the distance between the interferometer phase centres, $H$ is altitude of the interferometer, and $\bar{\beta}$ is the mean grazing angle. This expression describes the baseline decorrelation assuming registration of the two signals so that the footprints overlap [3, 4] (i.e., when $\tau$ is chosen so that the interferometer axis is steered to point at the common footprint). Note, in the radar literature it is more common to model the compressed pulse as a sinc function so that the sinc in (13) is replaced with a triangular function [5–7].

A difference (see Table 1) between InSAS and InSAR (especially spaceborne InSAR) is the grazing angle $\bar{\beta}$ (measured from the horizontal). InSAS is commonly deployed in shallow waters (such as harbours) and thus the grazing angles are small, typically 5–30 degrees, where the Kirchhoff approximation is poor [8]. Airborne InSAR uses a similar geometry but for spaceborne InSAR the grazing angles are steeper, typically 30–60 degrees and thus the decorrelation is greater. Another key difference is that the relative bandwidth of InSAS systems is much greater than InSAR (apart from a few VHF airborne systems such as CARABAS [9]). This results from

| | InSAR (space) | InSAR (air) | InSAS |
|---|---|---|---|
| Propagation speed | fast | fast | slow |
| Incidence angle | small | large | large |
| Relative bandwidth | small | small | large |
| Noise | receiver | receiver | environment |
| Footprint shift | small | small | significant |
| Wavenumber shift | significant | significant | insignificant |

Table 1: Key differences between InSAR and InSAS. The footprint shift is compared to the range resolution while the wavenumber shift is compared to the wavenumber bandwidth.

the desire of high range resolution given the slow speed of acoustic signals in water, the availability of broadband transducers, and no restrictions on usage of the underwater acoustic spectrum. Indeed, it is not uncommon to have a sonar with an octave bandwidth; thus the product $f_0 T_p$ is much smaller for InSAS than InSAR. However, this has little effect on the baseline decorrelation since the baseline $D$ is chosen to minimise baseline decorrelation. The disadvantage of a large relative bandwidth is that accurate co-registration is required to reduce decorrelation due to the footprint shift. To see this, let's assume that the look angles are equal so $\eta_{x1} = \eta_{x2} = \eta_x$ and thus there is no baseline decorrelation. The resulting correlation coefficient due to the footprint shift is

$$\rho_{12}(t,\tau) = \exp\left(\mathrm{j}\Phi(t)\right) M\left(0,\tau\right), \tag{14}$$

where

$$M(0,\tau) = \frac{\int_{-\infty}^{\infty} p\left(\frac{\bar{x}_2 - x}{c}\eta_x\right) p^*\left(\frac{\bar{x}_1 - x}{c}\eta_x - \tau\right) \mathrm{d}x}{\int_{-\infty}^{\infty} \left|p\left(\frac{x}{c}\eta_x\right)\right|^2 \mathrm{d}x}. \tag{15}$$

# 4 Height estimation

Interferometric height estimation is a super-resolution technique that makes the assumption that there is only a single dominant scattering patch for each slant range (thus multipath and layover are assumed negligible). Essentially the task is to estimate the terrain height $z$ that maximises the correlation coefficient between the echo signals. For each height guess $z$ at a slant range $r = ct/2$ the footprint centres $\bar{x}_h$, grazing angles $\beta_h$, and wavenumber scale factors $\eta_{xh}$ can be determined. The echo signals can then be time scaled, shifted, and correlated using

$$\rho_{12}(t,\tau,\eta) = \frac{\mathrm{E}\left[d_2(\eta t) d_1^*(t-\tau)\right]}{\sqrt{\mathrm{E}\left[\left|d_1(t-\tau)\right|^2\right] \mathrm{E}\left[\left|d_2(\eta t)\right|^2\right]}}, \tag{16}$$

where $\eta = \eta_{x1}/\eta_{x2}$. The height estimate $\hat{z}$, is the height guess that maximises the correlation coefficient. This can be expressed as a search:

$$\hat{z}(t) = \arg\max_z \left|\rho_{12}(t,\tau(z),\eta(z))\right|. \tag{17}$$

Since this is computationally expensive, a simpler approach is to ignore the time scaling (or to make a correction based on the expected height) and to just estimate the time delay between the two signals that maximises the correlation coefficient:

$$\hat{\tau}(t) = \arg\max_\tau \left|\rho_{12}(t,\tau)\right|, \tag{18}$$

$$= \arg\max_\tau \frac{\left|\mathrm{E}\left[d_1^*(t) d_2(t-\tau)\right]\right|}{\sqrt{\mathrm{E}\left[\left|d_1(t)\right|^2\right] \mathrm{E}\left[\left|d_2(t-\tau)\right|^2\right]}}, \tag{19}$$

where $\mathrm{E}\left[.\right]$ is the expectation operator. The delay estimate is then converted to a height estimate through a geometric mapping.

Equation (19) requires averaging over an ensemble of independent echoes. While a number of along-track samples can be averaged, this degrades the along-track resolution. Additional averaging can be obtained at the expense of range resolution by assuming that the signals are ergodic and performing a time-correlation over an observation time $T$:

$$\hat{\tau}(t) = \arg\max_\tau \frac{\left|\int_{-\infty}^{\infty} u_2(t,t') u_1^*(t,t'-\tau)\mathrm{d}t'\right|}{\sqrt{\int_{-\infty}^{\infty} \left|u_2(t,t')\right|^2 \mathrm{d}t' \int_{-\infty}^{\infty} \left|u_1(t,t')\right|^2 \mathrm{d}t'}}, \tag{20}$$

where

$$u_h(t,t') = d_h(t+t') \,\mathrm{rect}\left(\frac{t'}{T}\right). \tag{21}$$

The correlation can be performed in the frequency domain using

$$\hat{\tau}(t) = \arg\max_\tau \frac{\left|\int_{-\infty}^{\infty} U_2(t,f) U_1^*(t,f) \exp\left(\mathrm{j}2\pi f\tau\right) \mathrm{d}f\right|}{\sqrt{\int_{-\infty}^{\infty} \left|U_2(t,f)\right|^2 \mathrm{d}f \int_{-\infty}^{\infty} \left|U_1(t,f)\right|^2 \mathrm{d}f}}, \tag{22}$$

where

$$U_h(t,f) = \int_{-\infty}^{\infty} u_h(t,t') \exp\left(-\mathrm{j}2\pi f t'\right) \mathrm{d}t'. \tag{23}$$

Time delay estimation theory shows that the variance of the time delay estimate about the true delay can be reduced using generalised correlation [10]. Here each signal is filtered by a filter response $W_h(f)$ (or equivalently one of the signals can be filtered by $W(f) = W_1(f)W_2(f)$) to minimise the variance of the time delay estimates. The optimal filter response to minimise the variance is [11]

$$W(f) = \frac{\left|\gamma_{12}(f)\right|^2}{\left|S_{12}(f)\right| \left[1 - \left|\gamma_{12}(f)\right|^2\right]}, \tag{24}$$

where $S_{12}(f)$ is the cross power spectral density between $u_1$ and $u_2$, and $\gamma_{12}(f)$ is the cross spectral coherence:

$$\gamma_{12}(f) = \frac{S_{12}(f)}{\sqrt{S_1(f) S_2(f)}}, \tag{25}$$

$$\approx \frac{\mathrm{E}\left[U_2(f) U_1^*(f)\right]}{\sqrt{\mathrm{E}\left[\left|U_1(f)\right|^2\right] \mathrm{E}\left[\left|U_2(f)\right|^2\right]}}. \tag{26}$$

Here $S_1(f)$ and $S_2(f)$ are the power spectral densities of $u_1$ and $u_2$. Note if both channels have uncorrelated

additive noise with the same power spectrum $S_{nn}(f)$, the cross spectral coherence becomes

$$\gamma_{12}(f) = \frac{S_{12}(f)}{\sqrt{(S_1(f) + S_{nn}(f))\,(S_2(f) + S_{nn}(f))}}. \quad (27)$$

Assuming a rough scattering surface with stationary statistics, the power spectral density of the pulse compressed echoes are proportional to the energy spectral density of the compressed pulse signal $p(t)$ weighted by the beam patterns and the footprint response. Since the vertical beam patterns are wide to span a broad swath, the slight difference in look angle results in minimal difference in beam pattern response. The difference in look angle does, however, result in a small variation in the footprint response, known as the wavenumber shift [12]. The wavenumber shift is a narrowband approximation of the scaling of the scattered wavenumber spectrum. This results in a temporal frequency shift $\Delta f$ between equivalent features in the echo power spectra, given by

$$\Delta f \approx -\frac{fD}{H} \sin\bar{\beta} \tan\left(\bar{\beta} + \alpha\right) \cos\left(\bar{\beta} - \xi\right), \quad (28)$$

where $\alpha$ is the local terrain tilt for the footprint of interest. The wavenumber prefiltering [12] suggested to reduce the InSAR phase variance is essentially a form of generalised correlation. However, since the frequency shift is so small (otherwise the baseline decorrelation would be unacceptably large), wavenumber prefiltering is only useful for narrowband InSAR. It is more important for a broadband InSAS system to compensate for the wavenumber scaling. Care is required with the interpolation so that the small gain is not lost by interpolation noise during the time scaling.

Using the spectral weighting given by (24), the Cramér-Rao lower bound (CRLB) for the time delay variance is given by [11]

$$\sigma_\tau \geq \left[ T \int_{-\infty}^{\infty} (2\pi f)^2 \frac{|\gamma_{12}(f)|^2}{1 - |\gamma_{12}(f)|^2} \mathrm{d}f \right]^{-1/2}. \quad (29)$$

This shows that the greater the signal bandwidth (and thus the broader $\gamma_{12}(f)$), and the longer the observation time $T$, the smaller the variance of the delay $\sigma_\tau^2$ (and thus the depth) estimates. However, the longer the observation time $T$ (the extent of the correlation window), the lower the time (and thus range) resolution. Thus there is a tradeoff between resolution and the variance of the bathymetry estimates. This translates to a trade-off between across-track resolution and height accuracy.

InSAR systems are primarily narrowband and thus the CRLB of the estimated time delay using the signal phase is almost identical to the CRLB obtained using a time domain correlation. Thus the time delay can be estimated from the phase of the Hermitian product of the complex baseband signals. While the footprint shift is not significant for narrowband signals, it should be minimised by co-registering the signals before phase estimation. However, this requires an initial estimate of the terrain height or an initial delay estimate.

Estimating the phase has a computational advantage since it avoids computing the correlation and a search for the correlation peak. The disadvantage is that the time delay estimate is ambiguous since the phase can only be estimated modulo $2\pi$ and thus phase unwrapping techniques are required to reduce the ambiguity. The unambiguous time delay interval can be extended using a lower frequency (but with a degradation in accuracy) or by employing additional receivers (multiple baseline) [13]. It can also be extended by increasing the signal bandwidth [14]. Once the signal bandwidth is comparable with half the centre frequency, ambiguities can be avoided and phase unwrapping is unnecessary.

The time delay estimates can be improved by combining multiple estimates. As mentioned before, the variance of the estimate of $\tau$ is reduced by averaging the time correlations over neighbouring along-track positions, although this reduces the along-track resolution. This is equivalent to a maximum likelihood phase filter [15] when the signals are narrowband or accurately co-registered to compensate for the footprint shift [16]. Since electromagnetic propagation is so much faster than acoustic propagation, InSAR systems are better sampled in the along-track direction than InSAS. Thus it is common for InSAR to average over more along-track looks than InSAS and conversely for InSAS to average over more range samples than InSAR.

When there are more than two receivers the time delay estimate can be further improved by averaging the signal correlations, inversely weighted by the expected variances [17]. An interferometer with additional receivers also allows additional arrival angles to be estimated for each slant-range and thus can be used to mitigate the effects of layover [18] and multipath [19].

The CRLB of the time delay estimate using correlation depends on the the second moment of the normalised echo energy density spectrum:

$$\beta_0^2 = \frac{\int_0^\infty f^2 |P(f)|^2 \mathrm{d}f}{\int_0^\infty |P(f)|^2 \mathrm{d}f}. \quad (30)$$

This is related to the rms signal bandwidth $\beta$ and centre frequency $f_0$ through the identity [20]:

$$\beta_0^2 = \beta^2 + f_0^2. \quad (31)$$

So if we define the signal quality factor (Q) as the ratio of the centre frequency to rms bandwidth,

$$Q = \frac{f_0}{\beta} \quad (32)$$

then the second moment can be expressed in terms of the centre frequency and $Q$:

$$\beta_0 = f_0 \sqrt{1 + \frac{1}{Q^2}}. \quad (33)$$

Thus for narrowband systems with $Q \gg 1$ then $\beta_0 \approx f_0$ and hence there is little improvement performing a correlation over narrowband phase estimation (using the phase of the Hermitian product of the echo signal complex envelopes). This assumes that the SNR is sufficiently high so that the phase does not wrap. The disadvantage of narrowband phase estimation is that the delay estimate is ambiguous and phase unwrapping is required to reduce the ambiguities.

With InSAS it is common to correlate the complex envelopes of the echo signals rather than the real signals. This is more computationally efficient but the delay estimate using the correlation envelope is poor (the CRLB is inversely proportional to $\beta$ instead of $\beta_0$). The estimate can be improved using the phase at the correlation peak [21]; the resulting CRLB of the delay estimate is inversely proportional to $f_0$. This is close to optimal for narrowband systems but for broadband systems with low $Q$ the echo signals should be correlated after remodulating the complex envelopes to the centre frequency.

# 5 Conclusions

The key difference between InSAR and InSAS is the relative bandwidth. As a result, the narrowband InSAR algorithms are not applicable unless the InSAS signals are sub-banded and treated as a number of a narrowband estimates. A small improvement in the correlation coefficient can be obtained using generalised correlation, where the signals are filtered to maximise the coherence at each frequency. A slightly higher correlation coefficient can be obtained by time scaling one of the two signals (equivalent to remapping the slant range data to a common ground plane and thus compensating for the wavenumber spectrum scaling). However, unless a search is performed, this requires an estimate of the terrain height.

# References


[1] G. Jin and D. Tang, "Uncertainties of differential phase estimation associated with interferometric sonars," *IEEE J. Ocean. Eng.*, vol. 21, pp. 53–63, Jan. 1996.

[2] D. Jackson and M. Richardson, *High-frequency seafloor acoustics*. Springer, 2007.

[3] X. Lurton, "Swath bathymetry using phase difference: Theoretical analysis of acoustical measurement precision.," *IEEE J. Ocean. Eng.*, vol. 25, pp. 351–363, July 2000.

[4] J. S. Bird and G. K. Mullins, "Analysis of swath bathymetry sonar accuracy," *IEEE J. Oc. Eng.*, vol. 30, pp. 372–390, Apr. 2005.

[5] F. K. Li and R. M. Goldstein, "Studies of multibaseline spaceborne interferometric synthetic aperture radars," *IEEE Trans. Geosci. Remote Sens.*, vol. 28, pp. 88–97, Jan. 1990.

[6] E. Rodriguez and J. M. Martin, "Theory and design of interferometric synthetic aperture radars," *IEE Proc.—Part F*, vol. 139, pp. 147–159, Apr. 1992.

[7] R. Bamler and P. Hartl, "Topical review: Synthetic aperture radar interferometry," *Inverse Problems*, vol. 14, pp. R1–R54, Aug. 1998.

[8] J. M. Restrepo and S. T. McDaniel, "Two models for the spatially covariant field scattered by randomly rough pressure-release surfaces with Gaussian spectra," *J. Ac. Soc. Am.*, vol. 87, pp. 2033–2043, May 1990.

[9] L. M. H. Ulander and P. Frölind, "Ultra-wideband SAR interferometry," *IEEE Trans. Geosci. Remote Sens.*, vol. 36, pp. 1540–1550, Sept. 1998.

[10] C. H. Knapp and G. C. Carter, "The generalised correlation method for estimation of time delay," *IEEE Trans. Acoust., Speech, Signal Process.*, vol. 24, pp. 320–327, Aug. 1976.

[11] A. H. Quazi, "An overview on the time delay estimate in active and passive systems for target localization," *IEEE Trans. Acoust., Speech, Signal Process.*, vol. 29, pp. 527–533, June 1981.

[12] F. Gatelli, A. M. Guarnieri, F. Parizzi, P. Pasquali, C. Prati, and F. Rocca, "The wavenumber shift in SAR interferometry," *IEEE Trans. Geosci. Remote Sens.*, vol. 32, pp. 855–865, July 1994.

[13] G. Corsini, M. Diani, F. Lombardini, and G. Pinelli, "Simulated analysis and optimization of a three-antenna airborne InSAR system for topographic mapping," *IEEE Trans. Geosci. Remote Sens.*, vol. 37, pp. 2518–2529, Sept. 1999.

[14] R. Lanari, G. Fornaro, D. Riccio, M. Migliaccio, K. P. Papathanassiou, J. R. Moreira, M. Schwäbisch, L. Dutra, G. Puglisi, G. Franceschetti, and M. Coltelli, "Generation of digital elevation models by using SIR-C/X-SAR multifrequency two-pass interferometry: The Etna case study," *IEEE Trans. Geosci. Remote Sens.*, vol. 34, pp. 1097–1114, Sept. 1996.

[15] D. C. Ghiglia and M. D. Pritt, *Two-dimensional phase unwrapping: Theory, algorithms, and software*. New York, NY, USA: John Wiley and Sons, 1998.

[16] T. O. Sæbø, R. E. Hansen, and H. J. Callow, "Height estimation on wideband synthetic aperture sonar: Experimental results from InSAS-2000," in *MTS/IEEE OCEANS 2007*, 2007.

[17] M. P. Hayes, "Results of a multiple-baseline interferometric synthetic aperture sonar in shallow water," in *IVCNZ'06, Image and Vision Computing New Zealand*, (Great Barrier Island), 2006.

[18] F. Lombardini, M. Montanari, and F. Gini, "Reflectivity estimation for multibaseline interferometric radar imaging of layover extended sources," *IEEE Trans. Signal Process.*, vol. 51, pp. 1508–1519, June 2003.

[19] M. P. Hayes, "Multipath reduction with a three element interferometric synthetic aperture sonar," in *Proc. Seventh Euro. Conf. Underwater Acoust. (ECUA)*, (Delft, The Netherlands), pp. 1151–1156, ECUA, July 2004.

[20] A. W. Rihaczek, *Principles of High-Resolution Radar*. New York: M$^{c}$Graw-Hill, 1969.

[21] T. O. Sæbø, R. E. Hansen, and H. J. Callow, "Height estimation on wideband synthetic aperture sonar: Experimental results from InSAS-2000," in *MTS/IEEE OCEANS'05 USA*, (Washington DC, USA), Sept. 2005.